revista mexicana de física 27 no. 2 (1981) 143-167

MAGNETIZATION OF CYLINDRICAL HARD SUPERCONDUCTORS IN LONGITUDINALLY APPLIED MAGNETIC FIELDS

T.Akachi, R. Barrio

Instituto de Investigaciones en Materiales

Universidad Nacional Autónoma de México

and

G.Ramírez

Instituto de Física

Universidad Autónoma de San Luis Potosí

(recibido 3 junio, 1980)

ABSTRACT

On the basis of the critical state model, and using as its equation $J_c H_i^{\gamma} = \alpha$, the magnetization of cylindrical hard superconductors is calculated. The external magnetic field is applied parallel to the axis of symmetry of the sample. It is shown that there are three types of magnetization cycle curves that depend of the maximum applied magnetic field. It is demonstrated how to determine the parameters α and γ for any experimental magnetization curve.

RESUMEN

Partiendo del modelo del estado crítico y usando como su ecuación $J_c H_i^{\gamma} = \alpha$, se calcula la magnetización de superconductores duros de geometría cilíndrica cuando el campo magnético externo se aplica paralelo al eje de simetría. Se muestra que hay tres tipos de curvas cíclicas de magnetización que dependen del valor máximo del campo magnético aplicado. Se demuestra como determinar los parámetros α y γ de las curvas de magnetización experimentales.

I. INTRODUCTION

As it is well known, superconductors can be classified in two large groups, namely type I and type II. Magnetization measurements have played a very important role in determining the behavior of superconductors and in particular in their classification.

The main magnetic properties of type I superconductors can be easily described in the case of a long cylindrical sample with its axis parallel to the applied magnetic field H. Magnetic measurements show that the superconductor is a perfect diamagnet, a property known as the Meissner effect. In the superconducting state, there is no magnetic flux inside the material because surface currents circulate to give the specimen a magnetization exactly equal and opposite to the applied field. This negative magnetization disappears when the applied field strength reaches the critical value H_c and the superconductor becomes normal. For a pure specimen this behavior is reversible. The general properties of type I superconductors are well explained by the BCS microscopic theory[1].

Consider now a long cylindrical type II superconductor, again with its axis parallel to the applied field H. The total exclusion of the field from the sample (Meissner effect) occurs only for values of H smaller than H_{c1}, the lower critical magnetic field. Above H_{c1} the flux begins to rise internally, but remains less than the external flux. The normal state is reached at the field H_{c2}, the upper critical magnetic field, at which the internal flux becomes equal to the external flux. The region $H_{c1} < H < H_{c2}$, called the mixed state, is threaded by a large number of filaments of normal material lying parallel to the applied field and each carrying the quantum unit of flux. The filaments are surrounded by current vortices and repel each other so that they tend to be spread evenly through the mass in a regular pattern known as the Abrikosov lattice. The magnetization of type II superconductors is a thermodynamically stable state, reversible and independent of sample size. The theory of the magnetic behavior of ideal type II superconductors was developed by Ginzburg-Landau[2], Abrikosov[3] and Gor'kov[4] (GLAG theory).

For type II superconductors having chemical and physical inhomogeneities exceeding atomic dimensions, the experimental magnetization shows characteristics that are different from those predicted by the GLAG theory. These superconductors show lower and upper critical fields; that is, there is a mixed state, but the magnetization curve is irreversible showing a hysteresis loop that is dependent on the sample size. For an ideal defect-free sample of a type II superconductor in the mixed state, the flux filaments threading the sample are free to move, subject only to their mutual repulsive interactions and to a viscous drag, and any nonuniform distribution of flux filaments disappears quickly. However, for nonideal type II superconductors the flux filaments are pinned or trapped by defects in the structure of the material and give rise to an internal flux gradient. Such defects can be voids, normal inclusions, grain boundaries, compositional variations, dislocations, etc. In general, type II superconductors with the behavior described above are called hard superconductors and in particular those with high H_{c2} values are called high field superconductors.

The first phenomenological model to explain the magnetic behavior of hard superconductors was proposed by Bean[5] and further developed by Kim et al.[6], and is called the critical state model. The basic premise of this model is that there is a limiting macroscopic superconducting current density $J_c(H)$ that a hard superconductor can carry; and, further, that any electromotive force, however small, will induce this full current to flow locally. On the basis of this picture, there is always a full current flow J_c perpendicular to the external field H, except in those regions that have never felt the magnetic field. The sense of the currents depends on the sense of the electromotive force associated with the last local change of field. Bean[5] considered, as a first approximation, a current density independent of H and found, in a static magnetization experiment with a sintered V_3Ga sample, a rather detailed agreement for fields below 10 kOe. On the other hand, Kim et al.[6] reported a series of experiments on Nb-Zr, Nb_3Sn and V_3Ga specimens, covering a wide range of fields, and found good agreement with the critical state model predictions using a field dependent current density $J_c = \alpha/(H+B_o)$, where α and B_o are constant parameters.

Silcox and Rollins[7] have calculated the magnetization of hard superconductors considering the pinning force due to defects in the structure of the material and the interaction force between flux filaments. They were able to deduce the irreversible behavior and the size dependence of the magnetization curve. It can be shown[8] that the equation that gives the mean flux threading the specimen, derived by them, can be reduced to the critical equation, $J_c B = \text{const.}$ Following the approach taken by Silcox and Rollins, Yasukōchi et at.[8] found that the critical state equation that satisfactorily describes their experimental data on a Nb-Zr specimen, was $J_c B^{1/2} = \text{const.}$ On the other hand, Fietz et al.[9] proposed the critical equation $J_c B = \alpha(e^{-\beta B} + \gamma)$. Each one of the empirically chosen equations agrees quite well with the experimental data obtained by each group. Thus, it can be concluded that the critical state model is a satisfactory description.

This paper deals with the magnetization of cylindrical hard type II superconductors specimens, with the external field H applied parallel to the axis of symmetry of the sample. As the critical state equation it is proposed

$$J_c H_i^{\gamma} = \alpha(T) , \tag{1}$$

where the temperature dependent parameter $\alpha(T)$ is a quantity related to the pinning strength of the flux quanta and the parameter γ gives the power dependence of the critical current density J_c on the internal magnetic field H_i of the sample. In principle the parameter γ can take any real value, but the observed behavior of hard superconductors is well described by taking γ in the range $0 \leq \gamma \leq 1$.

Let us consider the response of the superconducting specimen to changes in the applied field. Ampère's law for cylindrical symmetry and for the critical state model reduces to

$$\frac{dH_i}{dr} = \begin{cases} 0, & \text{in regions where there is no field ,} \\ \pm \frac{4\pi}{c} J_c, & \text{in regions where there are fields ,} \end{cases} \tag{2}$$

where the sign is fixed by Lenz's law. Now, combining Eq.(1) and Eq.(2) and the boundary condition $H = H_i$ at the surface of the cylinder, we can calculate the internal field distribution in terms of H and r, for the different field regions. It can be shown that an increment of the applied field in a virgin sample causes a magnetic flux to penetrate inside the sample to a penetration depth Δ, yielding an internal field distribution, as is indicated schematically in Fig.1. The field profile depends on the value of the parameter γ. The current flows in the superficial layer of thickness Δ. For a sufficiently large applied field, $H = H^*$, the front of the field profile reaches the center line of the cylinder and currents flow through the entire volume of the specimen. Let us now consider what happens when the field is lowered from the maximum applied field, or peak field H_0. As the field is lowered, the surface feels an emf oppositely directed to the one felt as the field was increasing, and this causes the flux to move out of the sample (see Fig.2). Starting at the surface of the sample and moving inwards, there is a reversal of the local current flow. When the field reaches $H = 0$, the field distribution is that shown in Fig.2 and there is a trapped (or remanent) flux.

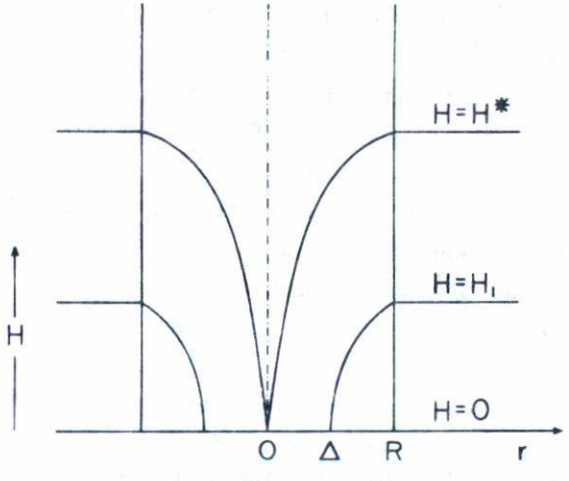

Fig.1 Schematic representation of the internal field distribution for a cylindrical hard superconductor specimen of radius R when the external field H, applied parallel to the axis of the cylinder, is increased from H=0 to H=H*.

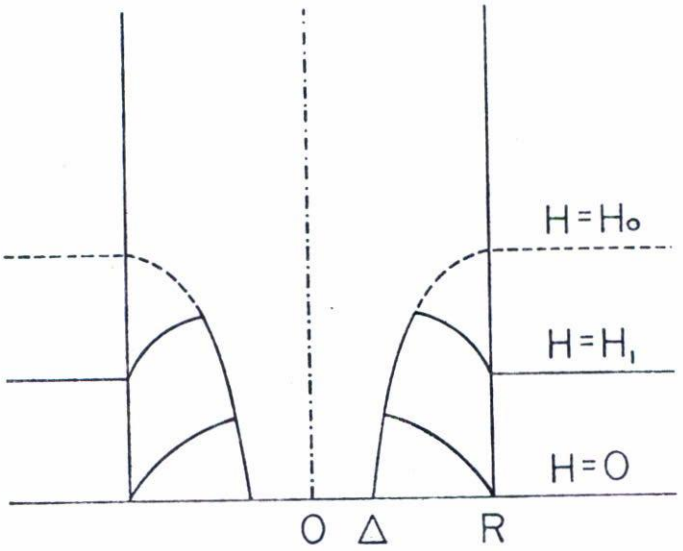

Fig.2 Schematic representation of the internal field distribution when the external field is decreased from the maximum applied field H_0 to H=0.

It can be seen that for a given hard superconducting sample for which γ has some fixed value, there are three different field profiles for the remanent flux, that depend on the value of the peak field H_0, as is illustrated in Fig.3. The first one (see Fig. 3a) occurs when H_0 is not sufficiently high in order that the flux front can reach the center line of the cylindrical sample. In that case, when the field is lowered from $H=H_0$ to H=0, the resultant remanent field profile is as that shown schematically in Fig.3a . The second one occurs when H_0 is such that the flux front reaches the center line of the cylinder but not so high as to completely rub out the increasing field profile when the field is lowered to zero, the field profiles for the remanent flux is as shown in Fig.3b. The third one occurs when, H_0 is sufficiently high so that when the field is lowered to zero, the remanent field profile does not exhibit any trace of the increasing field profile, as is shown schematically in Fig.3c. Therefore, these three different remanent field profiles lead to a three distinct types of mag-

netization curves that depend on the value of the peak field H_o. Our aim is to calculate explicitly, by the use of the critical state equation (1), the three different symmetric magnetization cycle curves for cylindrical hard superconductor samples with the external applied field parallel to the axis of symmetry.

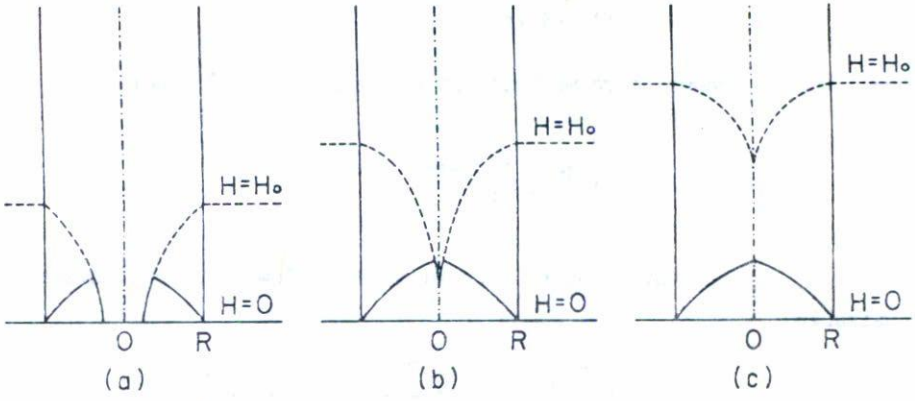

Fig. 3 Schematic representation of the three possible remanent internal field distributions.

II. CALCULATION OF THE MAGNETIZATION

The magnetization M is defined by the following equation:

$$-4\pi M = \int (H - H_i)\, dV \Big/ \int dV, \tag{3}$$

where both integrals are over the volume of the specimen, H is the external applied field and H_i the internal field. To perform the integration, H_i must be stated in terms of H and r for the different field regions of interest. This is done by the pertinent combination of Eqs. (1) and (2).

For the first stage of the magnetization, that is, when the applied field is increased from 0 to $H \leq H^*$, we have

$$H_i(r) = \begin{cases} 0, & 0 \leq r \leq \Delta, \\ [H^{\gamma+1} - (\gamma+1)\frac{4\pi}{c}\alpha(R-r)]^{1/(\gamma+1)}, & \Delta \leq r \leq R, \end{cases} \tag{4}$$

where we assume that $H_i = H$ at $r = R$. The penetration depth Δ is the value of the radius at which H_i becomes zero, that is

$$\Delta = R - \frac{H^{\gamma+1}}{(\gamma+1)\,\alpha\, 4\pi/c} . \tag{5}$$

Now, when Δ becomes zero we have, by definition, $H = H^*$; therefore

$$H^* = \left[(\gamma+1)\frac{4\pi}{c}\alpha R \right]^{1/(\gamma+1)} . \tag{6}$$

It is convenient to introduce the following dimensionless variables:

$$\rho = \frac{r}{R} ; \qquad h = \frac{H}{H^*} ; \qquad m = \frac{M}{H^*} ; \qquad h_n = \frac{H_n}{H^*} \tag{7}$$

(where n represents any subscript that appears in the context). Using these quantities, Eqs. (3) and (4) can be written as

$$-4\pi m = \int (h - h_i)\, dv \Big/ \int dv \tag{8}$$

and

$$h_i(\rho) = \begin{cases} 0 , & 0 \leq \rho \leq \delta , \\ [h^{\gamma+1} - 1 + \rho]^{1/(\gamma+1)}, & \delta \leq \rho \leq 1 , \end{cases} \tag{9}$$

where

$$dv = \rho d\rho d\varphi dz$$

and

$$\delta = \Delta/R = 1 - h^{\gamma+1} \tag{10}$$

a) Magnetization Cycle I.

Let us now calculate the normalized magnetization cycle corresponding to the case when the residual magnetization profile is like that of Fig.3a; that is, when the normalized peak field h_o satisfies $0 \leq h_o \leq 1$. Fig.4 illustrates schematically the normalized internal field distribution (only the right hand side of the cross section of the cylinder is shown) for the different stages of the magnetization cycle. Following this scheme we have:

Step 1. The external field increases from $h = 0$ to $h = h_o$. The flux front penetrates into the sample up to a point marked by δ_o. For $0 \leq h \leq h_o$, the normalized internal field distribution is given by Eq.(9). Substituting Eq. (9) in Eq. (8) and performing the integration, we have that the corresponding normalized magnetization is

$$-4\pi m = h - \frac{2(\gamma+1)}{(\gamma+2)} h^{\gamma+2} \left[1 - \frac{\gamma+1}{2\gamma+3} h^{\gamma+1} \right]. \tag{11}$$

Step 2. Once the field reaches h_o, the field is diminished to $h = 0$. The magnetic flux begins to move out of the sample. From Eqs.(1) and (2) it is found that for $h_o \leq h \leq 0$ the distribution of the normalized internal fields is

$$h_i(\rho) = \begin{cases} 0 , & 0 \leq \rho \leq \delta_o , \\ [h_o^{\gamma+1} - 1 + \rho]^{1/(\gamma+1)}, & \delta_o \leq \rho \leq \delta' , \\ [h^{\gamma+1} + 1 - \rho]^{1/(\gamma+1)}, & \delta' \leq \rho \leq 1 , \end{cases} \tag{12}$$

where

$$\delta_o = 1 - h_o^{\gamma+1} ; \quad \delta' = 1 - \frac{1}{2}\left(h_o^{\gamma+1} - h^{\gamma+1} \right) . \tag{13}$$

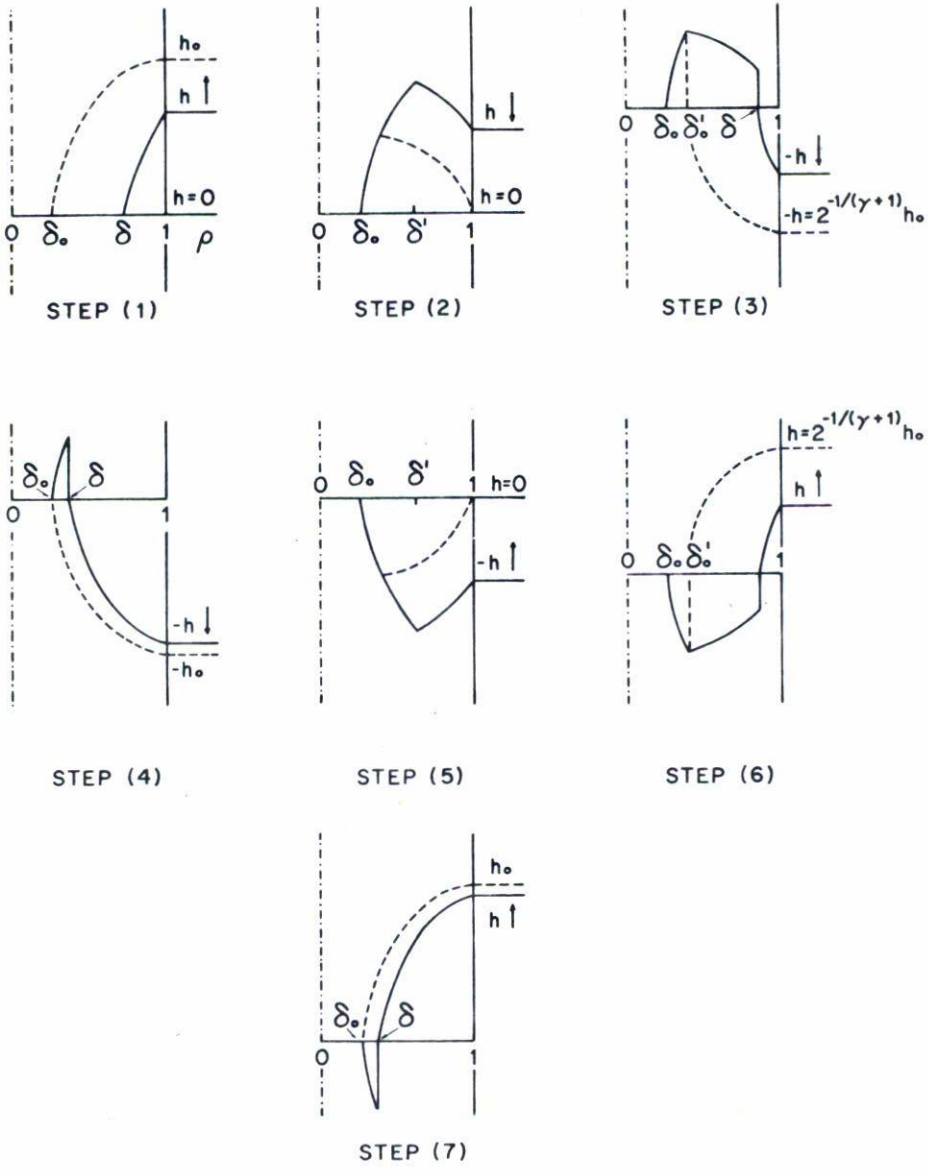

Fig.4 Schematic representation of the normalized internal field distribution for the different stages of the magnetization cycle, for the case when $h_o \leq 1$ (only the right hand side of the cross section of the cylinder is shown).

The magnetization is calculated again substituting Eqs. (12) in Eq. (8), giving

$$-4\pi m = h - \frac{2(\gamma+1)}{(\gamma+2)} \left\{ \left[\frac{h_o^{\gamma+1} + h^{\gamma+1}}{2} \right]^{(\gamma+2)/(\gamma+1)} \left[2 - h_o^{\gamma+1} + h^{\gamma+1} \right] \right.$$

$$\left. - h^{\gamma+2} \left[1 + \frac{\gamma+1}{2\gamma+3} h^{\gamma+1} \right] \right\} . \qquad (14)$$

Step 3. The applied field is now negatively increased from $h = 0$ to $h = -2^{-1/(\gamma+1)} h_o$. The field distribution is

$$h_i(\rho) = \begin{cases} 0 , & 0 \le \rho \le \delta_o \quad , \\ [\, h_o^{\gamma+1} - 1 + \rho \,]^{1/(\gamma+1)} , & \delta_o \le \rho \le \delta_o' \quad , \\ [\, 1 - \rho \,]^{1/(\gamma+1)} , & \delta_o' \le \rho \le \delta \quad , \\ -[\, |h|^{\gamma+1} - 1 + \rho \,]^{1/(\gamma+1)} , & \delta \le \rho \le 1 \quad , \end{cases} \qquad (15)$$

where

$$\delta_o' = 1 - \frac{1}{2} h_o^{\gamma+1} . \qquad (16)$$

The calculated magnetization is

$$-4\pi m = -|h| - \frac{2(\gamma+1)}{(\gamma+2)} \left[\left(\frac{h_o^{\gamma+1}}{2} \right)^{(\gamma+2)/(\gamma+1)} \left(2 - h_o^{\gamma+1} \right) \right.$$

$$\left. - |h|^{\gamma+2} \left(2 - |h|^{\gamma+1} \right) \right] . \qquad (17)$$

Step 4. The applied field h is now $-2^{-1/(\gamma+1)} \; h_o \le h \le -h_o$, the field distribution is

$$h_i(\rho) = \begin{cases} 0 , & 0 \le \rho \le \delta_o , \\ [h_o^{\gamma+1} - 1 + \rho]^{1/(\gamma+1)} , & \delta_o \le \rho \le \delta , \\ -[\,|h|^{\gamma+1} - 1 + \rho\,]^{1/(\gamma+1)} , & \delta \le \rho \le 1 , \end{cases} \qquad (18)$$

and for the magnetization we obtain

$$-4\pi m = -|h| - \frac{2(\gamma+1)}{(\gamma+2)} \left[\left(h_o^{\gamma+1} - |h|^{\gamma+1} \right)^{(\gamma+2)/(\gamma+1)} \left(1 - \frac{(\gamma+1)}{(2\gamma+3)} h_o^{\gamma+1} - \frac{(\gamma+2)}{(2\gamma+3)} |h|^{\gamma+1} \right) - |h|^{\gamma+2} \left(1 - \frac{(\gamma+1)}{(2\gamma+3)} |h|^{\gamma+1} \right) \right] . \qquad (19)$$

To complete the magnetization cycle, we have to calculate the normalized field distributions and the normalized magnetizations corresponding to steps 5, 6 and 7 of Fig.4. The normalized field distributions can be obtained from those of steps 2, 3 and 4, by means of reflections through the ρ axis. The expressions for the normalized magnetizations for steps 5, 6 and 7 can be obtained from Eqs. 14, 17 and 19, respectively, considering the effect of performing the inversion through the origin of the graph of $-4\pi m$ against h.

Fig. 5 shows a curve of a magnetization cycle, calculated from the above equations, for the arbitrary values $h_o = 0.85$ and $\gamma = 0.3$.

b) Magnetization Cycle II

When the remanent magnetization is like that of Fig.3b, the magnetization cycle is calculated when the normalized peak field h_o satisfies $1 \le h_o \le 2^{1/(\gamma+1)}$. The normalized internal field distribution, for this case, is represented schematically, step by step, in Fig. 6.

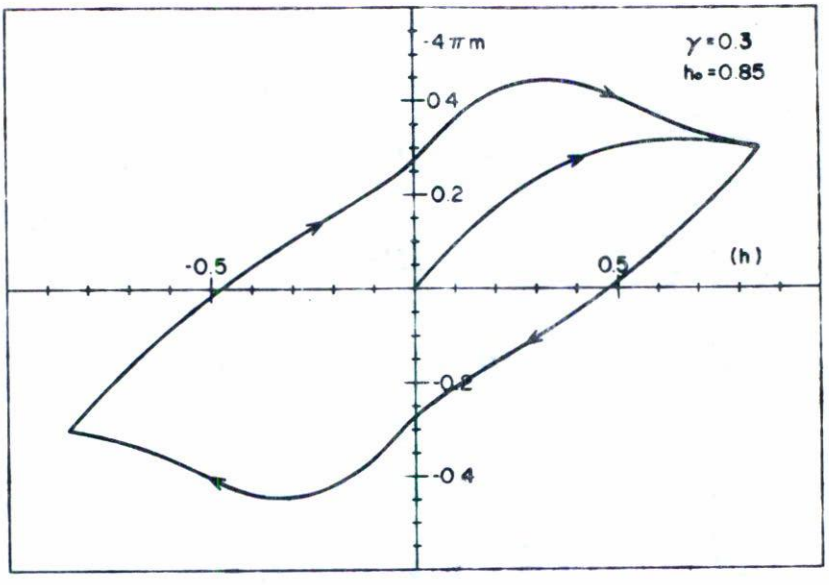

Fig.5 Normalized magnetization cycle curve for $h_0 = 0.85$ and $\gamma = 0.3$.

The calculation of the complete symmetric normalized magnetization curve can be done in a way similar to that of cycle I. The results are:

Step 1. Increasing field for $0 \leq h \leq 1$.

The field distribution and the corresponding magnetization are the same as those of cycle I, that is Eqs. (9) and (11) respectively.

Step 2. Increasing field for $1 \leq h \leq h_0$.

The field distribution is given by

$$h_i(\rho) = [h^{\gamma+1} - 1 + \rho]^{1/(\gamma+1)} , \qquad 0 \leq \rho \leq 1 , \tag{20}$$

and the corresponding magnetization is

$$-4\pi m = h - \frac{2(\gamma+1)}{(\gamma+2)} \left[h^{\gamma+2} \left(1 - \frac{(\gamma+1)}{(2\gamma+3)} h^{\gamma+1} \right) + \frac{(\gamma+1)}{(2\gamma+3)} [h^{\gamma+1} - 1]^{(2\gamma+3)/(\gamma+1)} \right] . \tag{21}$$

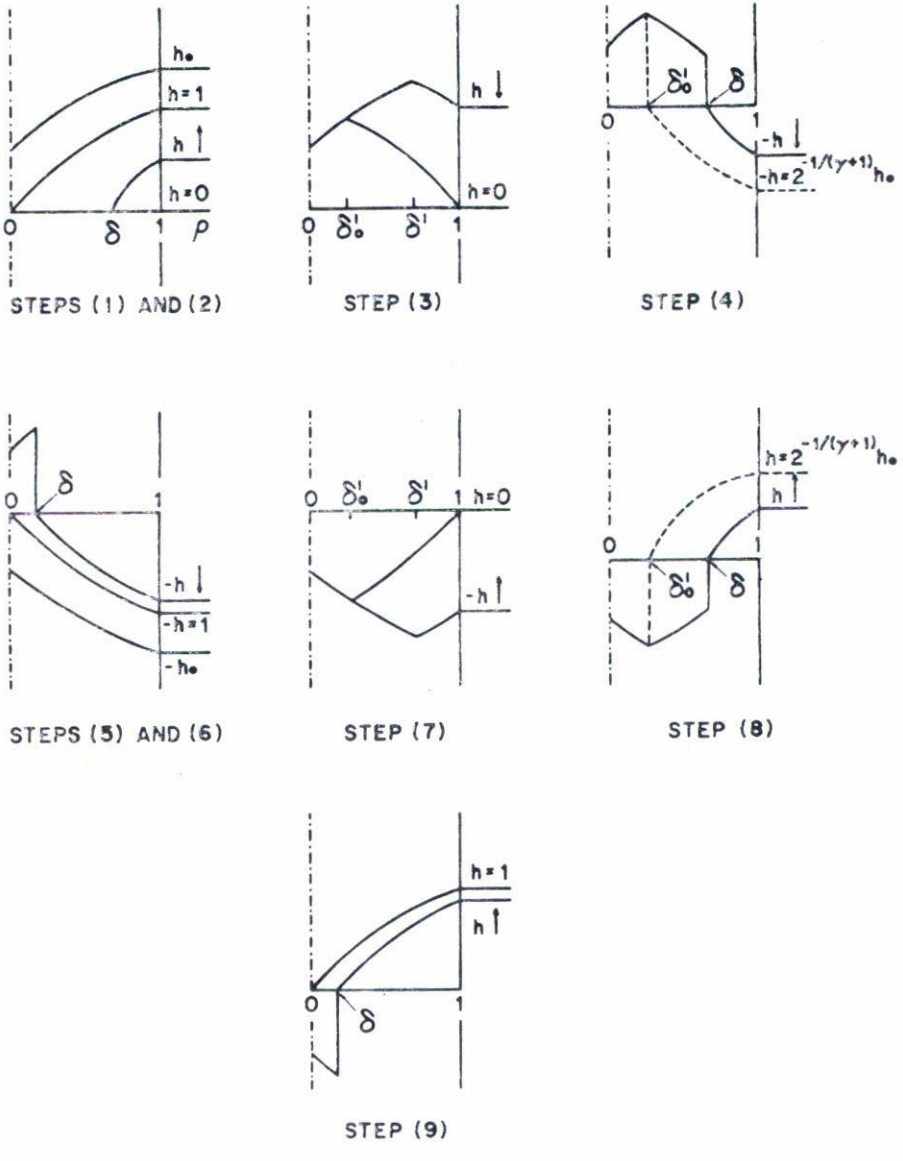

Fig.6 Schematic representation of the normalized internal field distribution for the different stages of the magnetization cycle for the case when $1 \leq h_o \leq 2^{1/(\gamma+1)}$ (only the right hand side of the cross section of the cylinder is shown).

Step 3. Decreasing field for $h_o \leq h \leq 0$.
In this case we have

$$h_i(\rho) = \begin{cases} [\, h_o^{\gamma+1} - 1 + \rho\,]^{1/(\gamma+1)}, & 0 \leq \rho \leq \delta' \\ [\, h^{\gamma+1} + 1 - \rho\,]^{1/(\gamma+1)}, & \delta' \leq \rho \leq 1 \end{cases} , \tag{22}$$

where δ' is given by Eq. (13). The resulting magnetization is

$$-4\pi m = h - \frac{2(\gamma+1)}{(\gamma+2)} \left[\left(\frac{h_o^{\gamma+1} + h^{\gamma+1}}{2} \right)^{(\gamma+2)/(\gamma+1)} \left(2 + h^{\gamma+1} - h_o^{\gamma+1} \right) \right.$$

$$\left. - h^{\gamma+2} \left(1 + \frac{(\gamma+1)}{(2\gamma+3)} h^{\gamma+1} \right) + \frac{(\gamma+1)}{(2\gamma+3)} \left(h_o^{\gamma+1} - 1 \right)^{(2\gamma+3)/(\gamma+1)} \right] . \tag{23}$$

Step 4. Increasing field negatively for $0 \leq h \leq -2^{-1/(\gamma+1)} h_o$.

$$h_i(\rho) = \begin{cases} [\, h_o^{\gamma+1} - 1 + \rho\,]^{1/(\gamma+1)}, & 0 \leq \rho \leq \delta_o' \\ [\, 1 - \rho\,]^{1/(\gamma+1)}, & \delta_o' \leq \rho \leq \delta \\ -[\, |h|^{\gamma+1} - 1 + \rho\,]^{1/(\gamma+1)}, & \delta \leq \rho \leq 1 \end{cases} , \tag{24}$$

and

$$-4\pi m = -|h| - \frac{2(\gamma+1)}{(\gamma+2)}\left[\left(\frac{h_o^{\gamma+1}}{2}\right)^{(\gamma+2)/(\gamma+1)}\left(2 - h_o^{\gamma+1}\right)\right.$$

$$\left. + \frac{(\gamma+1)}{(2\gamma+3)}\left(h_o^{\gamma+1} - 1\right)^{(2\gamma+3)/(\gamma+1)} - |h|^{\gamma+2}\left(2 - |h|^{\gamma+1}\right)\right]. \tag{25}$$

Step 5. Increasing field negatively for $-2^{-1/(\gamma+1)}h_o \leq h \leq -1$.

$$h_i(\rho) = \begin{cases} [h_o^{\gamma+1} - 1 + \rho]^{1/(\gamma+1)}, & 0 \leq \rho \leq \delta, \\ -[|h|^{\gamma+1} - 1 + \rho]^{1/(\gamma+1)}, & \delta \leq \rho \leq 1, \end{cases} \tag{26}$$

and

$$-4\pi m = -|h| - \frac{2(\gamma+1)}{(\gamma+2)}\left[\left(h_o^{\gamma+1} - |h|^{\gamma+1}\right)^{(\gamma+2)/(\gamma+1)}\right.$$

$$\left(1 - \frac{(\gamma+1)}{(2\gamma+3)}h_o^{\gamma+1} - \frac{(\gamma+2)}{(2\gamma+3)}|h|^{\gamma+1}\right)$$

$$+ \frac{(\gamma+1)}{(2\gamma+3)}\left(h_o^{\gamma+1} - 1\right)^{(2\gamma+3)/(\gamma+1)}$$

$$\left. - |h|^{\gamma+2}\left(1 - \frac{(\gamma+1)}{(2\gamma+3)}|h|^{\gamma+1}\right)\right]. \tag{27}$$

We can observe in Fig.6 that steps 6, 7, 8 and 9 have the same normalized field distribution as those of steps 2, 3, 4 and 5, respectively, but with $-h$ instead of h. In the same way as we have done in cycle I, we have to do an inversion through the origin in order to obtain

the corresponding magnetization. Fig.7. shows a normalized magnetization cycle curve when $\gamma = 0.75$ and $h_o = 1.3$.

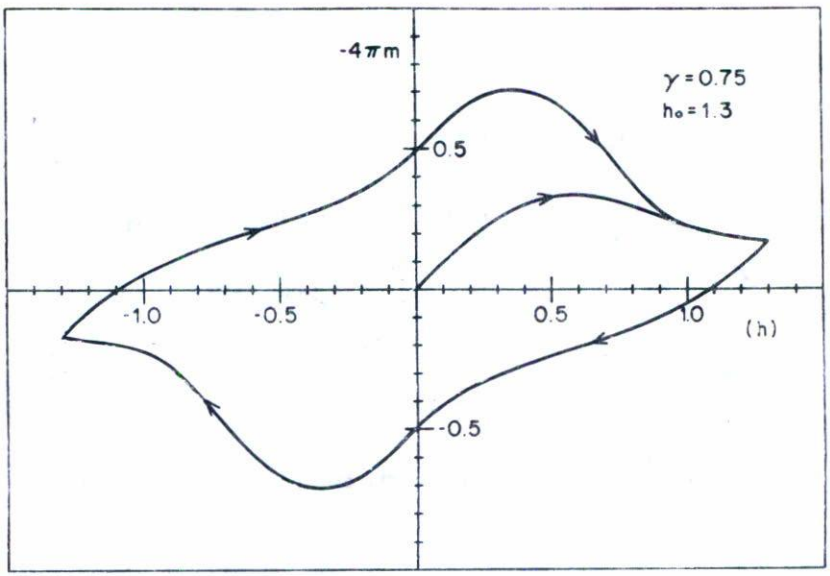

Fig.7 Normalized magnetization cycle curve for $h_o = 1.3$ and $\gamma = 0.75$.

c) Magnetization Cycle III

When $2^{1/(\gamma+1)} \leq h_o << h_{c2}$, we have a situation corresponding to a residual magnetization like that on Fig.3c. The normalized internal field distribution is illustrated in Fig. 8. The calculated results are as follows:

Step 1. Increasing field for $0 \leq h \leq h_o$.

The field distributions and the corresponding magnetization are the same as those of step 1 and 2 of cycle II.

Step 2. Decreasing field for $h_o \leq h \leq (h_o^{\gamma+1} - 2)^{1/\gamma+1}$.

The corresponding equations for field distributions and magnetization are Eqs. (22) and (23) of cycle II, respectively.

Step 3. Decreasing field for $(h_o^{\gamma+1} - 2)^{1/\gamma+1} \leq h \leq 0$.

For the field distributions we have

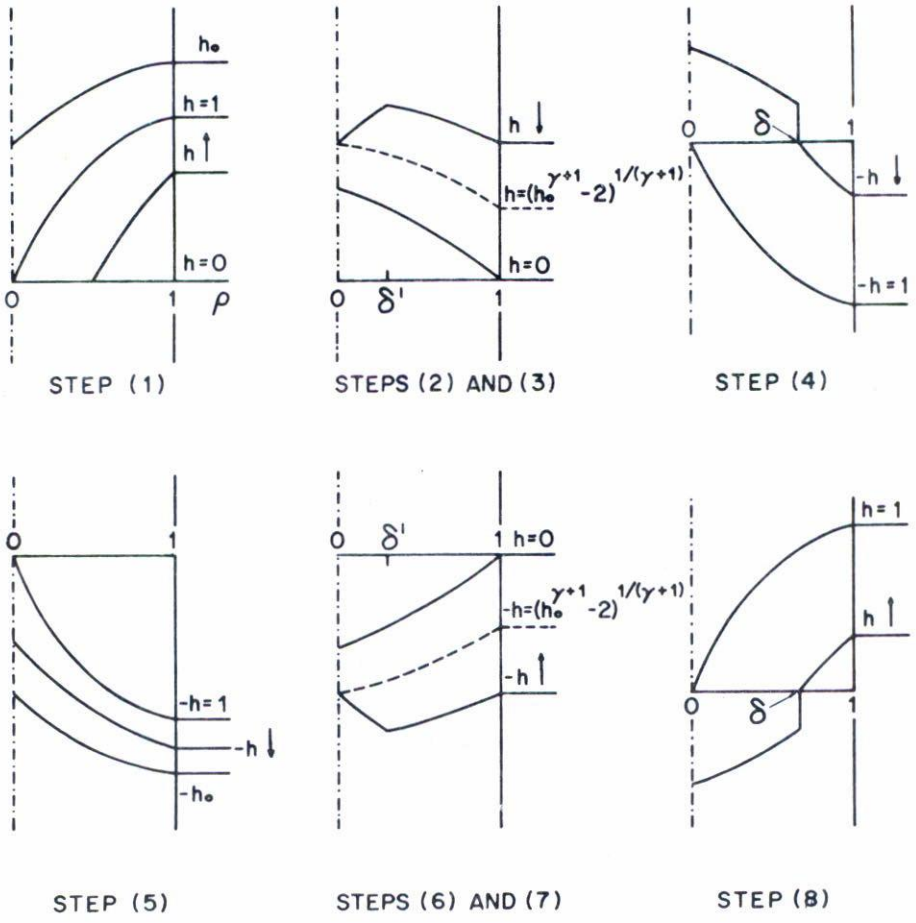

Fig.8 Schematic representation of the normalized internal field distribution for the different stages of the magnetization cycle for the case when $2^{1/(\gamma+1)} \leq h_0 << h_{c2}$ (only the right hand side of the cross section of the cylinder is shown).

$$h_i(\rho) = [h^{\gamma+1} + 1 - \rho]^{1/(\gamma+1)}, \qquad 0 \le \rho \le 1 , \tag{28}$$

and for the magnetization

$$-4\pi m = h + \frac{2(\gamma+1)}{(\gamma+2)} \left[h^{\gamma+2} \left(1 + \frac{(\gamma+1)}{(2\gamma+3)} h^{\gamma+1} \right) - \frac{(\gamma+1)}{(2\gamma+3)} \left(1 + h^{\gamma+1} \right)^{(2\gamma+3)/(\gamma+1)} \right]. \tag{29}$$

Step.4 Increasing field negatively for $0 \le h \le -1$.
We have

$$h_i(\rho) = \begin{cases} [1 - \rho]^{1/(\gamma+1)} , & 0 \le \rho \le \delta , \\ -[|h|^{\gamma+1} - 1 + \rho]^{1/(\gamma+1)} , & \delta \le \rho \le 1 , \end{cases} \tag{30}$$

and

$$-4\pi m = -|h| + \frac{2(\gamma+1)}{(\gamma+2)} \left[|h|^{\gamma+2} \left(2 - |h|^{\gamma+1} \right) - \frac{(\gamma+1)}{(2\gamma+3)} \right]. \tag{31}$$

Step 5. Increasing field negatively for $-1 \le h \le -h_0$.
We have

$$h_i(\rho) = -[|h|^{\gamma+1} - 1 + \rho]^{1/(\gamma+1)}, \qquad 0 \le \rho \le 1 , \tag{32}$$

and

$$-4\pi m = -|h| + \frac{2(\gamma+1)}{(\gamma+2)} \left[|h|^{\gamma+2} \left(1 - \frac{(\gamma+1)}{(2\gamma+3)} |h|^{\gamma+1} \right) + \frac{(\gamma+1)}{(2\gamma+3)} \left(|h|^{\gamma+1} - 1 \right)^{(2\gamma+3)/(\gamma+1)} \right]. \tag{33}$$

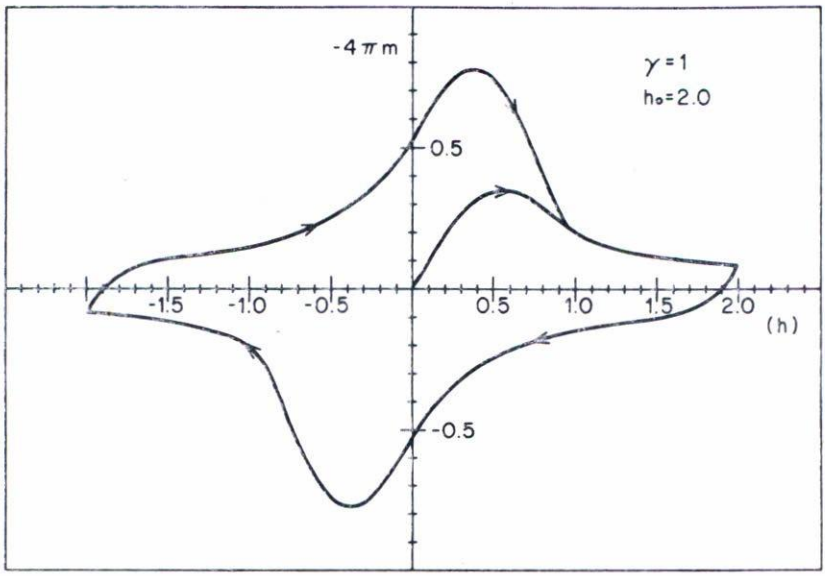

Fig.9 Normalized magnetization cycle curve for h_o=2.0 and γ =1.0 .

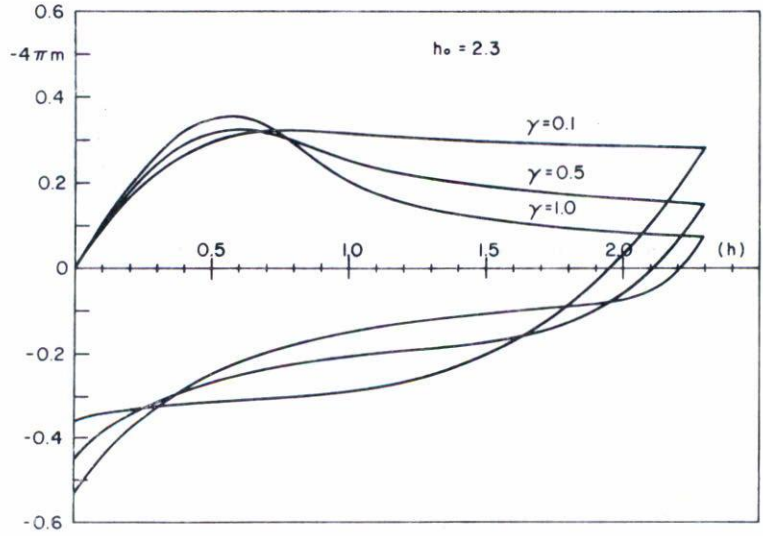

Fig.10 Three magnetization curves, corresponding to γ=0.1, γ=0.5 and γ= 1.0 whith h_o=2.3 . We observe that the normalized field h_{max}, the negative normalized meximum magnetization $-4\pi m_{max}$ and the remanent magnetization $4\pi m_R$ have, in each case, different values.

To complete the magnetization cycle, we have to calculate the normalized field distribution and the normalized magnetizations corresponding to steps 6, 7 and 8 of Fig.8. These calculations can be done from steps 2, 3 and 4, respectively, just as we have done in cycles I and II. A complete magnetization cycle for $\gamma = 1$ and $h_o = 2$, is shown in Fig.9 .

Fig.10 shows three magnetization curves for $\gamma = 0.1$, $\gamma = 0.5$ and $\gamma = 1.0$ with $h_o = 2.3$, when the field h increases from zero to h_o and goes back to zero. Among the features appearing in these curves we notice the strong dependence of the fall off of the curves, after passing through the maximum, on the parameter γ; that is, we find that the decay is bigger as γ increases. Also, the normalized maximum magnetization and the normalized field value at which it occurs depends on γ. From Eq.(11), taking the derivative of m with respect to h and equating it to zero, we obtain the normalized field h_{max} at which the normalized maximum magnetization $-4\pi m_{max}$ occurs; that is

$$h_{max}^{\gamma+1} = \frac{\gamma+2 - \sqrt{\gamma(\gamma+2)}}{2(\gamma+1)} \quad ; \tag{34}$$

substituting this value of h_{max} in Eq.(11) we have

$$-4\pi m_{max} = \frac{(\gamma+1)}{(2\gamma+3)} \left[1 + \sqrt{\frac{\gamma}{\gamma+2}} \right] \left[\frac{\gamma+2 - \sqrt{\gamma(\gamma+2)}}{2(\gamma+1)} \right]^{1/(\gamma+1)} . \tag{35}$$

Hence, we have that both h_{max} and $-4\pi m_{max}$ depend only on the parameter γ. Fig.11 and Fig.12 show the graphs of h_{max} and $-4\pi m_{max}$ against γ, respectively, for $0 \leq \gamma \leq 1$. Another characteristic we observe in Fig.10 is the dependence on γ of the normalized remanent magnetization $4\pi m_R$. Taking $h = 0$ in Eqs. (14), (23) and (29) we can obtain $4\pi m_R$, for any value of h_o. Fig.13 shows curves of $4\pi m_R$ as a function of h_o for $\gamma = 0$, $\gamma = 0.5$ and $\gamma = 1$. We have tat the remanent magnetization, for any value of γ, increases with increasing h_o, until h_o reaches the value $2^{1/(\gamma+1)}$, and that it becomes constant thereafter. This constant value will be large if γ is large.

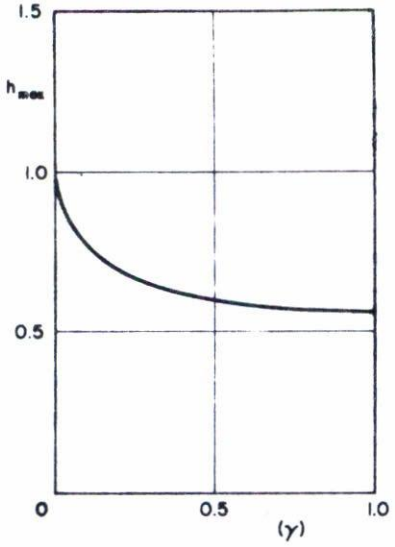

Fig. 11 Plot of h_{max} against γ $(0 \leq \gamma \leq 1)$.

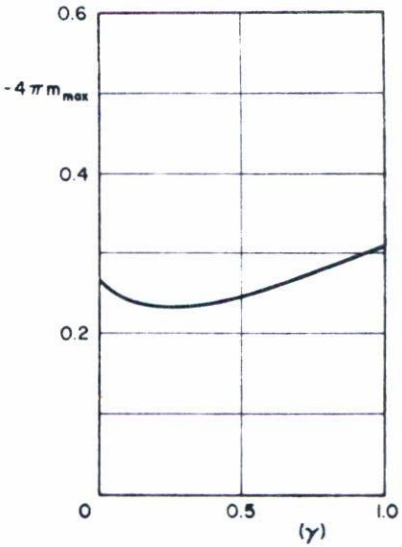

Fig. 12 Plot of $-4\pi m_{max}$ against γ $(0 \leq \gamma \leq 1)$.

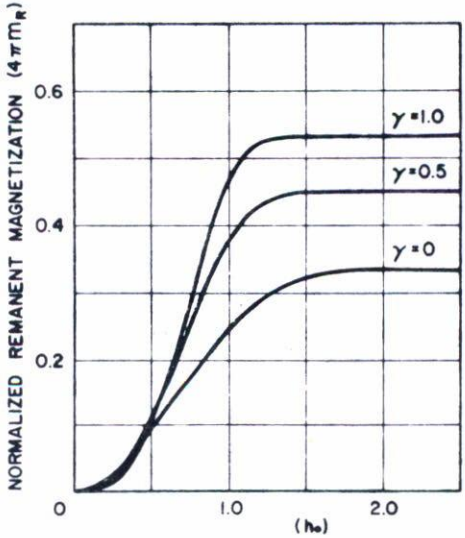

Fig. 13 The normalized remanent magnetization $4\pi m_R$ as a function of the normalized peak field h_o for $\gamma=0$, $\gamma=0.5$ and $\gamma=1.0$.

III PARAMETERS α AND γ

We shall consider now how to determine the values of the parameters α and γ for any particular experimental magnetization curve.

When a virgin hard superconductor sample is magnetized, the negative magnetization increases from zero, goes through a maximum and then decreases. This part of the magnetization is given by Eq.(11).The normalized field h_{max} at which the maximum normalized magnetization $-4\pi m_{max}$ occurs, is given by Eq.(34) as a function of the parameter γ. By definition $h_{max} = H_{max}/H^*$, where H_{max} is the external field at which maximum magnetization occurs. H_{max} can be measured from the particular experimental curve. Therefore we can obtain H^* in terms of H_{max} and γ.

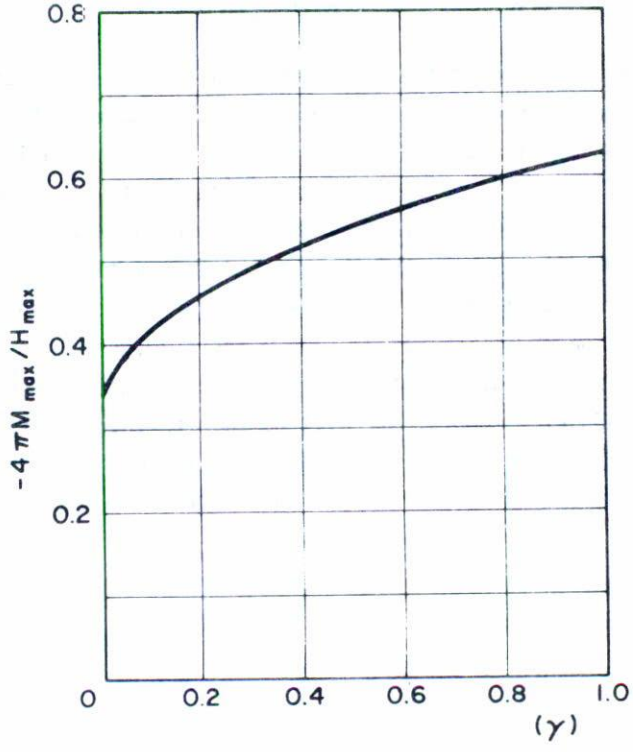

Fig.14 Plot of $-4\pi M_{max}/H_{max}$ against γ, for $0 \leq \gamma \leq 1$.

Putting $h = h_{max}$ in Eq.(11) and substituting its value from Eq.(34), we obtain

$$-\frac{4\pi m_{max}}{h_{max}} = -\frac{4\pi M_{max}}{H_{max}} = \frac{(\gamma+1)}{(2\gamma+3)}\left[1+\sqrt{\frac{\gamma}{\gamma+2}}\right]. \qquad (36)$$

The ratio $-4\pi M_{max}/H_{max}$ is plotted in Fig.14 as function of the parameter $\gamma(0\leq\gamma\leq 1)$. The value of this ratio can be calculated from the particular experimental curve, then the corresponding value of γ is obtained from the graph of Fig.14. Once γ is known we find immediately the value of H^* and from Eq.(16), the corresponding value of the parameter α.

IV CONCLUSIONS

We have demostrated that there exist three possible symmetric magnetization cycle curves, that depend on the value of the peak field h_0. We have calculated explicitly these three magnetization cycles on the basis of the critical state model, using as its equation $J_c H_i^{\gamma} = \alpha(T)$. We have found that some characteristics of the magnetization curve, such as the field h_{max} at which the negative maximum magnetization occurs, the negative maximum magnetization $-4\pi m_{max}$ and the remanent magnetization $4\pi m_R$, depend on the parameter γ. These facts suggest that there could possibly be a correlation between γ and the pinning centers existing in the superconducting sample. It will be interesting to perform a series of experiments, controlling the kind of pinning centers introduced into the sample, designed to find out if such correlation exists.

REFERENCES

1. J. Bardeen, L.N. Cooper, and J.R. Schrieffer, Phys. Rev. 108 (1957) 1175.
2. V.L.Ginzburg and L.D. Landau, Zh. Eksperim. i Teor. Fiz. 20 (1950) 1064.
3. A.A. Abrikosov, Zh. Eksperim. i Teor. Fiz. 32 (1957) 1442; Soviet Phys. JETP 5 (1957) 1174.
4. L.P. Gor'kov, Zh. Eksperim. i Teor. Fiz. 37 (1959) 1407; Soviet Phys. JETP 10 (1960) 998.
5. C.P. Bean, Phys. Rev. Letters 8 (1962) 250; Rev. Mod. Phys. 36 (1964) 31.
6. Y.B. Kim, C.F. Hempstead and A. R. Strnad, Phys. Rev. 129 (1963) 528.
7. J.Silcox and R.W. Rollins, Rev. Mod. Phys. 36 (1964) 52.
8. K. Yasukōchi, T. Ogasawara, N. Usui and S. Ushio, J.Phys. Soc. Japan 19 (1964) 1649.
9. W.A. Fietz, M.R. Beasley, J. Silcox and W.W.Webb, Phys. Rev. 136 (1964) A335.